

Time- and frequency-resolved determination of ultrafast energy transfer in optical Kerr measurements

Mengmeng Yue¹ · Jinhai Si¹ · Lihe Yan¹ · Yang Yu¹ · Xun Hou¹

Received: 2 September 2016 / Accepted: 26 December 2016 / Published online: 1 February 2017
© Springer-Verlag Berlin Heidelberg 2017

Abstract Transient energy transfer effect might occur in femtosecond pump–probe optical Kerr gate (OKG) measurements. Using time- and frequency-resolved two-dimensional pump–probe imaging spectroscopy, we are able to obtain the OKG spectra as a function of the delay time between pump and probe pulses. By analyzing the pump power dependence of the OKG spectra at different delay time, we find that due to the effect of transient energy transfer, the short-wavelength components of the OKG spectra are enhanced when the delay of the probe to pump pulse is positive, while the long-wavelength components increase when the delay is negative.

1 Introduction

Since the invention of ultrafast pulsed lasers, a number of pump–probe spectroscopic techniques have been developed for studying ultrafast transient phenomena in materials [1–6]. In conventional pump–probe measurements, several repetitions of pulses are required to obtain complete temporal information, as a scanning process is essential in the measurements. However, in cases where irradiation by ultrafast laser pulses induces irreversible changes in the samples, actual measurements become difficult. Although this problem can be solved in liquids where the samples can be refreshed by flowing, such an approach is not feasible

for some solid materials and some biochemical samples, where large sample quantities are not readily available [7–10]. To overcome this difficulty, time–frequency two-dimensional (2D) pump–probe imaging spectroscopy on a single-shot basis has been proposed for mapping the temporal and spectral information of the ultrafast phenomena simultaneously, which can be widely used in measuring some irreversible ultrafast processes [11–15].

As one of the key tools to investigate the nonlinear instantaneous process, femtosecond time-resolved optical Kerr gate (OKG) technique has been developed due to its great advantages include a wide wavelength range, ultrafast switching, and high precision [16, 17]. By combing with single-shot measurements, the femtosecond time- and frequency-resolved OKG technique has been used for imaging ultrafast transient signals and charactering ultrashort laser pulses [18, 19]. In the femtosecond time regime, however, the superposition of two coherent pulses might yield a spatially modulated distribution of the energy density, and the interaction with the sample would induce laser-induced transient gratings (LITG). Energy transfer between two beams by self-diffraction effect induced by LITG occurs during this process, which is dependent primarily on the field correlation time of the two incident pulses, does not reflect the nonlinear response time of the materials and decreases the signal-to-noise ratio in OKG measurements. So it is important to investigate the effect of transient energy transfer in femtosecond single-shot pump–probe optical Kerr measurements.

In this paper, we performed femtosecond single-shot pump–probe OKG measurements and obtained time–frequency two-dimensional (2D) image of the OKG signals in BI glass. The observed temporal and spectral properties of the OKG signals are in good agreement with those obtained through conventional OKG measurements. Transient

✉ Jinhai Si
jinhaisi@mail.xjtu.edu.cn

¹ Key Laboratory for Physical Electronics and Devices of the Ministry of Education and Shaanxi Key Lab of Information Photonic Technique, School of Electronics and Information Engineering, Xi'an Jiaotong University, Xi'an 710049, China

energy transfer from the pump beam to the probe beam induced by LITG effect was demonstrated by analyzing the pump power dependence of the OKG spectra at different delay times. The short-wavelength components of the OKG spectra were observed to increase when the delay time of the probe pulse to the pump pulse was set at a positive value. Conversely, when the delay time was set at a negative value, we observed an increase in the long-wavelength components of the OKG spectra.

2 Experimental

Figure 1 shows a schematic diagram of the single-shot experimental setup used for time–frequency 2D imaging of femtosecond OKG signals. A Ti: sapphire amplifier system emitting 65fs laser pulses with a central wavelength of 800 nm at a repetition rate of 1 kHz with horizontal linear polarization was used. The laser beam was split into a pump beam and a probe beam by a beam splitter. The pump pulse was passed through a $\lambda/2$ plate to change the polarization angle between the pump and probe pulses. The pump and probe beams were focused on a 1 mm-thick BI glass (prepared by melting Bi_2O_3 , B_2O_3 , SiO_2 and GeO_2 in the required proportions [20]) using cylindrical lenses of focal lengths of 40 and 15 mm, respectively. The pump and probe beams made an angle of 12° with each other at the vertical direction and their focal lines are spatially overlapped at the sample. Because of the finite vertical crossing angle, the arrival time of the pump and probe pulses differed, depending on the overlapping position on the sample. In other words, the delay time could be mapped spatially across the sample plane. After passing through the sample, the polarization of the probe pulse changes, and only the components polarized parallel to the analyzer placed behind the sample could be extracted. The OKG signal passing through the analyzer was imaged by a 4f system onto the entrance slit of an optical multichannel analyzer (OMA) comprising of a spectrograph, and coupled onto an

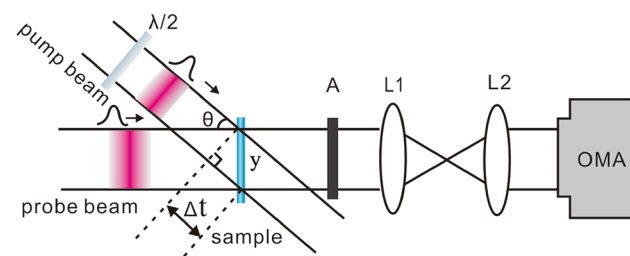


Fig. 1 Schematic diagram of the experimental setup, *A* analyzer, *L1*, *L2* lenses with focal lengths of 150 mm, *OMA* optical multichannel analyzer, *y* overlap position of the probe and pump beams on the sample, Δt delay time

intensified charge coupled device (ICCD) detector. Finally, a time- and frequency-resolved 2D OKG signal was imaged on the detector, the spectral information of which was analyzed by the spectrograph along the direction perpendicular to the slit, whereas the temporal information was recorded along the direction parallel to the slit. The relation between the time coordinate Δt and the spatial coordinate *y* can be expressed as:

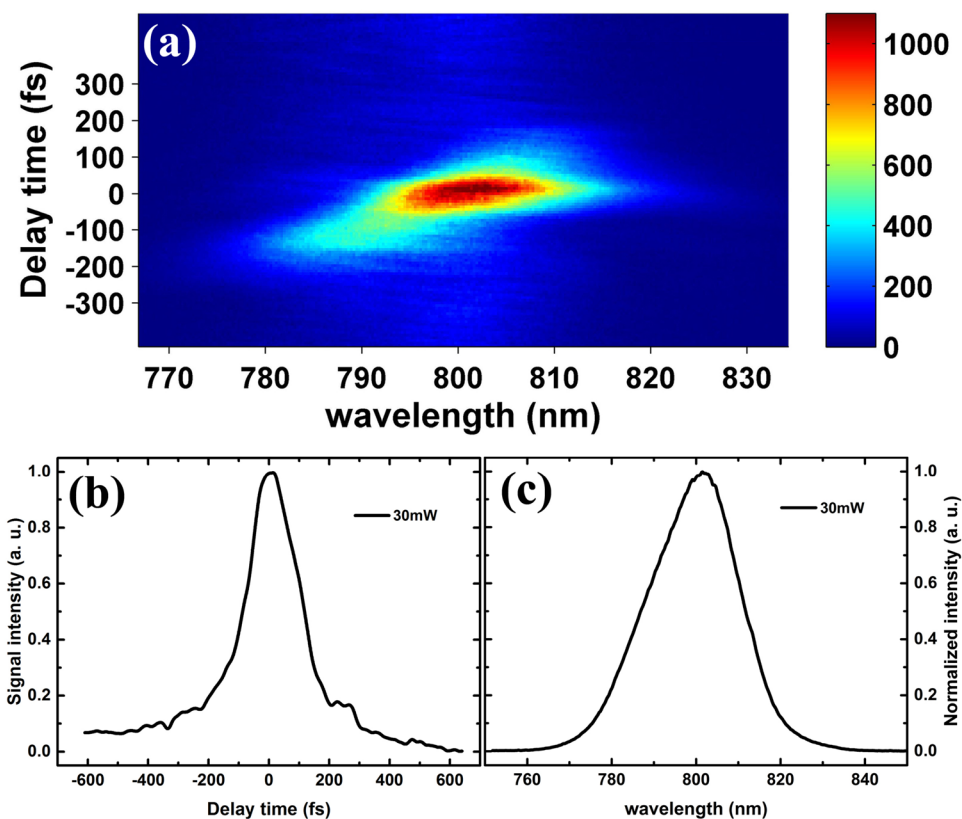
$$\Delta t = \frac{y \times \sin \theta}{c} \quad (1)$$

where *y* is the overlap position of the probe and pump beams on the sample, θ is the vertical angle between the pump and probe beams, and *c* refers to the speed of light in air. The time resolution of OKG imaging spectroscopy has a strong dependence on the sample thickness, the angle between the two beams and the laser pulse duration [21]. For our experimental conditions with a sample thickness of 1 mm, the time resolution is estimated to be approximately 250fs.

3 Results and discussion

Figure 2a shows the time- and frequency-resolved 2D image of an OKG signal obtained on the ICCD of the OMA acquired using the single-shot OKG measurement, with the pump and probe powers set at 30 and 5 mW, respectively. The image presents the signal intensity distribution as a function of wavelength (horizontal axis) and delay time (vertical axis). It is clearly observed that the image is tilted towards the bottom-right. In OKG measurements, the probe light field transmitted through the polarizer is a function of the delay time between the pump and probe pulses. In our experiments, taking into account the positive chirp characteristic of the laser, the long-wavelength components of the probe beam were transmitted and detected first, when the leading edge of the probe pulse overlapped with the trailing edge of the pump pulse. With the decreasing of the delay time, the probe pulse travelled in front of the pump pulse gradually, and the trailing edge with short-wavelength components were detected. This resulted in the observed tilt of the OKG signal image towards the bottom-right, as seen in Fig. 2a. The spectral and temporal traces could be easily obtained by integrating along the vertical and horizontal axes, respectively. The temporal trace shown in Fig. 2b, represents the OKG temporal behavior of BI glass. It covers a time region of approximately 250fs (estimated from the full-width at half maximum, FWHM). The temporal behavior of the OKG signals measured in our experiments is primarily decided by the time resolution of our imaging setup. The OKG signal has no obvious relaxation process, thus indicating the ultrafast response of BI glass due to

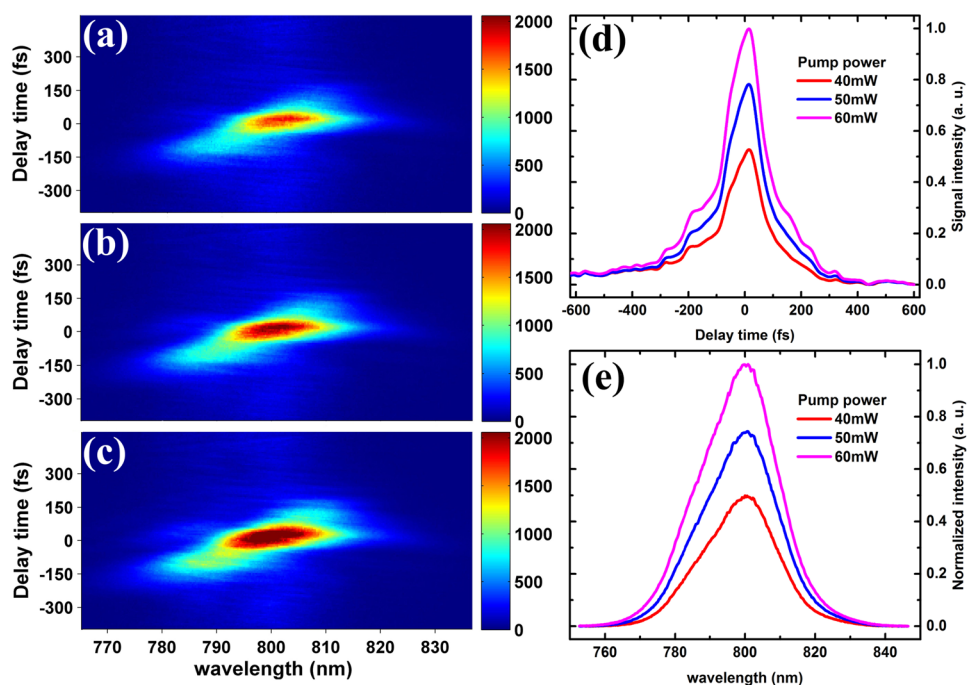
Fig. 2 **a** Time- and frequency-resolved 2D OKG image of BI glass obtained using single-shot measurements with the pump and probe power set at 30 and 5 mW, respectively. **b** Temporal trace obtained by integrating along the horizontal axis of **(a)**. **c** The spectral trace obtained by integration along the vertical axis of **(a)**



electronic processes [22, 23]. The spectral trace shown in Fig. 2c presents the normalized signal spectrum centered at a wavelength of 800 nm and covering a wavelength region of ~ 30 nm at FWHM.

The time- and frequency-resolved 2D OKG images of BI glasses were obtained at different pump power. Figure 3a–c present the acquired OKG images with the pump power increased to 40, 50, and 60 mW, respectively. It is observed

Fig. 3 Time- and frequency-resolved 2D OKG images of BI glass with pump power of **a** 40 mW, **b** 50 mW and **c** 60 mW. **d** Temporal traces obtained by integrating along the horizontal axes of **(a)**–**(c)**. **e** Spectral traces obtained by integrating along the vertical axes of **(a)**–**(c)**

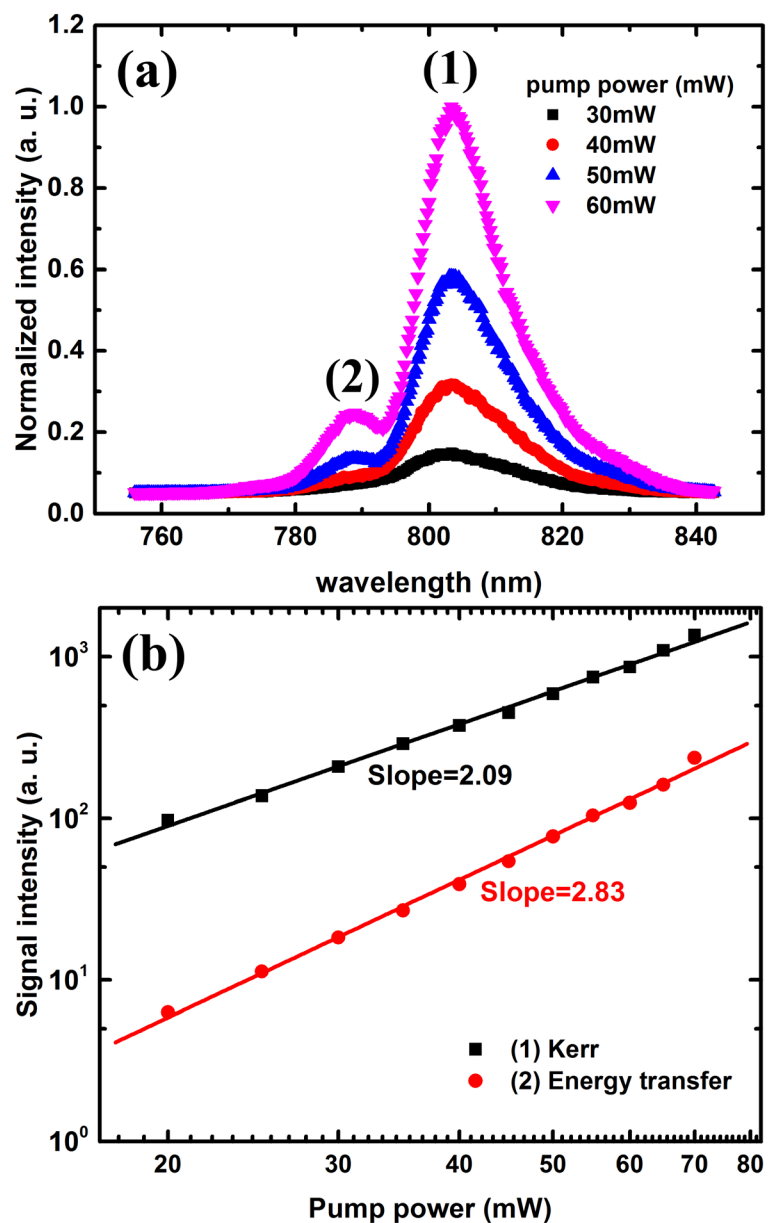


that the 2D OKG images become brighter with increasing pump power. Figure 3d, e show the temporal and spectral traces obtained by integrating along the horizontal and vertical axes of the respective OKG images. It is observed that, the intensities of the temporal and spectral traces increase with increasing pump power. However, irrespective of the signal intensity, the OKG signals exhibit no qualitative difference in their temporal and spectral behaviors with increasing pump power.

To investigate the pump power dependence of the OKG spectra, the OKG spectra at different delay time were reproduced by slicing off Fig. 2a along the horizontal direction in a single-shot measurement. Figure 4 presents the retrieved OKG signal spectra at different pump

powers with the delay time set at +150fs. It is clearly observed that the long-wavelength component with peak intensity at approximately 805 nm is transmitted through the analyzer in the presence of positive temporal delay. Furthermore, a second peak appears at approximately 790 nm when the pump power is increased. In OKG measurements, the probe pulse experiences transient birefringence induced by the pump pulse that allows the light to partially pass through the analyzer. When the delay time is positive, the leading edge with long-wavelength components of the probe pulse overlaps with the trailing edge of the pump pulse, and the OKG spectra are primarily distributed around the long-wavelength region. However, when the pump and probe pulses overlap

Fig. 4 **a** Retrieved spectra of OKG signals at different pump powers with the delay time set at +150fs. **b** Pump power dependence of energy transfer between the pump and probe pulses when the delay time kept at +150fs



spatially and temporally in the Kerr medium, the superposition of the two coherent pulses might yield a spatially modulated distribution of the energy density. As a consequence of the intensity-dependent effect the interference pattern of the two beams is transformed into a transient refractive-index grating. This grating would lead to a diffraction of the interfering beams resulting in an energy transfer between the two beams. At a temporal delay of +150fs, the probe pulse overlaps with the trailing edge with short-wavelength components of the pump pulse. As a result, the energy transfer from the pump pulse to the probe pulse will induce an enhancement of the short-wavelength components of the OKG signal spectra. Increasing the pump power, results in an enhanced diffraction efficiency of the refractive-index grating that in turn increases the transferred short-wavelength components in the OKG spectra.

To further confirm the influence of the energy transfer effect in OKG measurements, we studied the pump power dependence of intensities of peak (1) and peak (2) as denoted in Fig. 4a. The black squares and red circles in Fig. 4b show the pump power dependence of the peak (1) and peak (2) intensities in double logarithmic coordinates, respectively. The slope of the peak (1) was estimated to be 2.09, indicating that the signal shows a quadratic dependence on the pump power. This result agreed well with the fundamental of OKG measurements and some previous reports [24, 25]. As a comparison, the slope of the peak (2) intensity was estimated to be about 2.83. Therefore, it's reasonable to speculate that the rapid increasing of peak (2) was mainly attributed to the contribution of energy transfer from the pump beam in OKG measurements. Due to the joint contributions of energy transfer effect and OKG effect, the signal intensity at short wavelength region in OKG spectra (at positive delay) increased rapidly with increasing the pump power.

For a further understanding of the transient energy transfer process in femtosecond pump-probe OKG measurements, the spectra of OKG signals at negative and zero delay were retrieved from the time- and frequency-resolved 2D OKG images. Figure 5a, b present the retrieved OKG spectra at different pump powers with the delay times set at -150fs and zero, respectively. When the delay time is negative, the trailing edge with short-wavelength components of the probe pulse overlaps with the leading edge of the pump pulse, and the OKG spectra are primarily distributed around the short-wavelength region with peak intensities at approximately 790 nm, as seen in Fig. 5a. Due to diffraction at the transient refractive-index grating, the energy transfer from the pump pulse to the probe pulse induce an enhancement of the long-wavelength components of the OKG spectra. As a result, a peak appears at approximately 810 nm with increasing pump power.

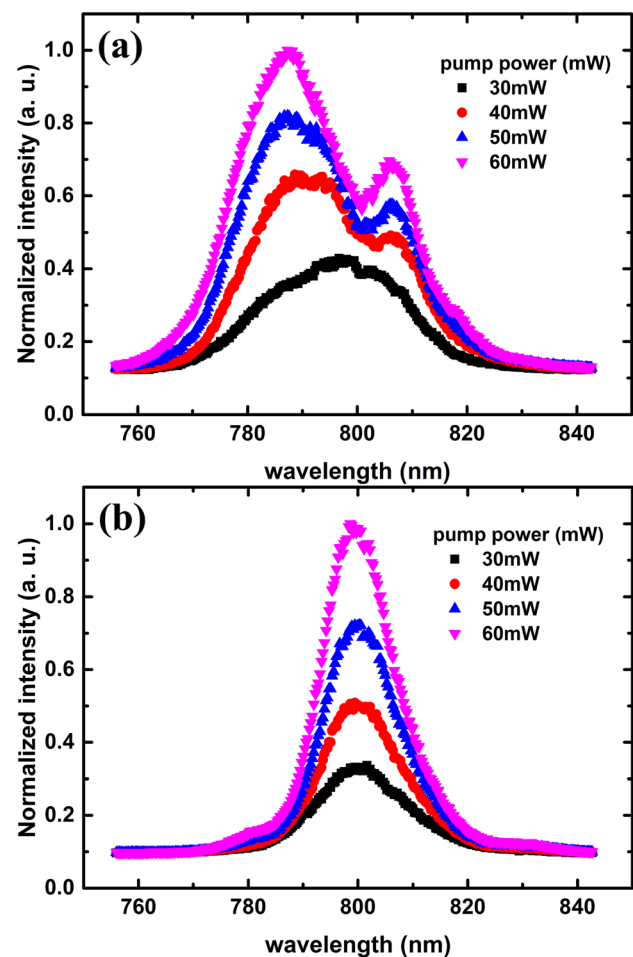


Fig. 5 a Retrieved spectra of OKG signals at different pump power with the delay time set at a -150fs and b zero

When the delay time is set at zero, the probe and pump pulses overlap completely. In this case, all the spectral components are transmitted through the analyzer, thus resulting in symmetric OKG spectra centered at a wavelength of 800 nm. Although energy transfer between the pump and probe pulses might occur, the transferred short- or long-wavelength components remain involved in producing the OKG spectra. As a result, no second peak is observed in the OKG spectra even increasing the pump power.

4 Conclusion

In summary, we have performed femtosecond single-shot pump-probe OKG measurements and obtained time-frequency 2D images of the OKG signals in BI glass. The observed temporal and spectral properties of the OKG signal are in good agreement with those acquired through conventional OKG measurements. By analyzing the pump power dependence of the OKG spectra at different delay

time, transient energy transfer from the pump beam to probe beam induced by LITG effect was demonstrated. The energy transfer from the pump pulse to the probe pulse induced an enhancement of the short-wavelength components of the OKG signal at positive temporal delay. Conversely, when the delay time was set at a negative value, the long-wavelength components of OKG spectra increased. For zero delay time, both the transmitted as well as transferred wave components were centered at a wavelength of 800 nm. This resulted in symmetric OKG spectra even increasing the pump power.

Acknowledgements This work was supported by the National Natural Science Foundation of China (Grant Nos. 61235003, 11474078 and 11674260), the Natural Science Basic Research Plan in Shaanxi Province of China (Program No. 2014JQ1024), the Research Fund for the Doctoral Program of Higher Education (Grant No. 20130201120025), and the Collaborative Innovation Center of Suzhou Nano Science and Technology.

References

1. R. Stoian, A. Rosenfeld, D. Ashkenasi, I.V. Hertel, N.M. Bulgakova, E.B. Campbell, Surface charging and impulsive ion ejection during ultrashort pulsed laser ablation. *Phys. Rev. Lett.* **88**, 097603 (1996)
2. T.Y. Chen, C.H. Hsia, H.S. Son, D.H. Son, Ultrafast energy transfer and strong dynamic non-condon effect on ligand field transitions by coherent phonon in γ -Fe₂O₃ nanocrystals. *J. Am. Chem. Soc.* **129**, 10829 (2007)
3. A.J. Sabbah, D.M. Riffe, Femtosecond pump-probe reflectivity study of silicon carrier dynamics. *Phys. Rev. B* **66**, 165217 (2002)
4. Z. Wang, B. Zeng, G. Li, H. Xie, W. Chu, F. He, Y. Liao, W. Liu, H. Gao, Y. Cheng, Time-resolved shadowgraphs of transient plasma induced by spatiotemporally focused femtosecond laser pulses in fused silica glass. *Opt. Lett.* **40**, 5726 (2015)
5. A. Azima, S. Dusterer, P. Radcliffe, H. Redlin, N. Stojanovic, W. Li, H. Schlarb, J. Feldhaus, D. Cubaynes, M. Meyer, J. Dardis, P. Hayden, P. Hough, V. Richardson, E.T. Kennedy, J.T. Costello, Time-resolved pump-probe experiments beyond the jitter limitations at FLASH. *Appl. Phys. Lett.* **94**, 144102 (2009)
6. H.L. Xu, A. Azarm, J. Bernhardt, Y. Kamali, S.L. Chin, The mechanism of nitrogen fluorescence inside a femtosecond laser filament in air. *Chem. Phys.* **360**, 171 (2009)
7. J.L. Pecourt, J. Peon, B. Kohler, Ultrafast internal conversion of electronically excited RNA and DNA nucleosides in water. *J. Am. Chem. Soc.* **122**, 9348 (2000)
8. E.A. McArthur, K.B. Eisenthal, Ultrafast excited-state electron transfer at an organic liquid/aqueous interface. *J. Am. Chem. Soc.* **128**, 1068 (2006)
9. M. M. Gabriel, J. R. Kirschbrown, J. D. Christesen, C. W. Pinion, D. F. Zigler, E. M. Grumstrup, B. P. Mehl, E. M. Cating, J. F. Cahoon, and J. M. Papanikolas, Direct imaging of free carrier and trap carrier motion in silicon nanowires by spatially-separated femtosecond pump-probe microscopy. *Nano. Lett.* **13**, 1336 (2013)
10. Y.S. Jang, J. Lee, S. Kim, K. Lee, S. Han, Y.J. Kim, S.W. Kim, Space radiation test of saturable absorber for femtosecond laser. *Opt. Lett.* **39**, 2831 (2014)
11. J.P. Geindre, P. Audebert, S. Rebibo, J.C. Gauthier, Single-shot spectral interferometry with chirped pulses. *Opt. Lett.* **26**, 1612 (2001)
12. Y. Minami, H. Yamaki, I. Katayama, and J. Takeda, Broadband pump-probe imaging spectroscopy applicable to ultrafast single-shot events. *Appl. Phys. E* **7**, 022402 (2014)
13. J. He, C. Zhu, Y. Wang, G. Cheng, K. Zou, D. Wu, X. Xie, A signal to noise ratio measurement for single shot laser pulses by use of an optical Kerr gate. *Opt. Express* **19**, 4438 (2011)
14. B. Yellampalle, K.Y. Kim, G. Rodriguez, J.H. Glowina, A.J. Taylor, Algorithm for high-resolution single-shot THz measurement using in-line spectral interferometry with chirped pulses. *Appl. Phys. Lett.* **87**, 211109 (2005)
15. J. Takeda, W. Oba, Y. Minami, T. Saiki, I. Katayama, Ultrafast crystalline-to-amorphous phase transition in Ge₂Sb₂Te₅ chalcogenide alloy thin film using single-shot imaging spectroscopy. *Appl. Phys. Lett.* **104**, 261903 (2014)
16. F. Wang, G. Dukovic, L.E. Brus, T. Heinz, Time-resolved fluorescence of carbon nanotubes and its implication for radiative lifetimes. *Phys. Rev. Lett.* **92**, 177401 (2004)
17. S. Matsuo, L.H. Yan, J.H. Si, T. Tomita, S. Hashimoto, Reduction of pulse-to-pulse fluctuation in laser pulse energy using the optical Kerr effect. *Opt. Lett.* **37**, 1646 (2012)
18. A.S. Shan, E. Weling, L. Knoesel, M. Bartels, Bonn, A. Nahata, G.A. Reider, T.F. Heinz, Single-shot measurement of terahertz electromagnetic pulses by use of electro-optic sampling. *Opt. Lett.* **25**, 426 (2000)
19. H. Sakaibara, Y. Ikegaya, I. Katayama, J. Takeda, Single-shot time-frequency imaging spectroscopy using an echelon mirror. *Opt. Lett.* **37**, 1118 (2012)
20. N. Sugimoto, H. Kanbara, S. Fujiwara, K. Tanaka, Y. Shimizu-gawa, and K. Hirao, Third-order optical nonlinearities and their ultrafast response in Bi₂O₃-B₂O₃-SiO₂ glasses. *JOSA B* **16**, 1904 (1999).
21. J. T. Fourkas, L. Dhar, K. A. Nelson, and R. Trebino, Spatially encoded single-shot ultrafast spectroscopies. *JOSA B* **12**, 155 (1995)
22. L. H. Yan, J. J. Yue, J. H. Si, S. Jia, F. Chen, and X. Hou, Polarization dependence of femtosecond optical kerr signals in bismuth glasses. *IEEE Photonics Technol. Lett.* **21**, 1606 (2009)
23. H. Inouye, K. Tanaka, I. Tanahashi, Y. Kondo, K. Hirao, Mechanism of a terahertz optical Kerr shutter with a gold nanoparticle system. *J. Phys. Soc. Jpn.* **68**, 3810 (1999)
24. H. Kanbara, S. Fujiwara, K. Tanaka, H. Nasu, K. Hirao, Third-order nonlinear optical properties of chalcogenide glasses. *Appl. Phys. Lett.* **70**, 925 (1997)
25. L.H. Yan, J.H. Si, Y.Q. Yan, F. Chen, X. Hou, Pump power dependence of femtosecond two-color optical Kerr shutter measurements. *Opt. Express* **19**, 11196 (2011)